NASA Technical Memorandum 101071

Composite Multilayer Insulations for Thermal Protection of Aerospace Vehicles

D. A. Kourtides and W. C. Pitts

February 1989

National Aeronautics and Space Administration

NASA Technical Memorandum 101071

Composite Multilayer Insulations for Thermal Protection of Aerospace Vehicles

D. A. Kourtides, Ames Research Center, Moffett Field, California
W. C. Pitts, Eloret Institute, Sunnyvale, California

February 1989

NASA

National Aeronautics and
Space Administration

Ames Research Center
Moffett Field, California 94035

COMPOSITE MULTILAYER INSULATIONS FOR THERMAL PROTECTION OF AEROSPACE VEHICLES

by

D. A. Kourtides
NASA Ames Research Center, Moffett Field, CA 94035

and

W. C. Pitts
Eloret Institute, Sunnyvale, CA

ABSTRACT

Composite, flexible multilayer insulation systems (MLI) were evaluated for thermal performance and compared with a fibrous silica (baseline) insulation system. Multilayer insulation systems are described, which consist of layers of metal foil alternating with ceramic scrim cloth or insulation and quilted together using ceramic thread. Three different types of reflective shields were also evaluated with various types of ceramic insulations. The first type was a stainless steel foil separated by aluminoborosilicate (ABS) scrim cloth. The insulations used in this multilayer system were either silica, ABS, or alumina felt. The second used aluminum foil in two different geometries. The foil layers were separated either by an ABS scrim cloth or by the insulation. The third type of reflective shield was an aluminized polyimide film. The film was placed on the bottom of a silica insulation. All three configurations contained an ABS cloth on the top and bottom of the entire insulation.

The merits of each insulation system were evaluated by their thermal response, or backface temperature increase (as measured in a thermal diffusivity apparatus), and their density. The multilayer insulations containing aluminum were the most efficient systems, measuring up to a 50% reduction in backface temperature increase, when compared with the silica baseline insulation system. However, these composite insulations were slightly heavier than the baseline. The insulation containing the aluminized polyimide also had a lower backface temperature with no weight penalty, when compared to the baseline system. A computer model was used to predict backface temperatures of similar insulations in the heating environment of a typical Aeroassist Orbital Transfer Vehicle for which these insulations may have an application.

1. INTRODUCTION

Aerospace vehicles, subject to high convective and radiative heating during atmospheric entry, require extremely efficient thermal protection systems capable of protecting the aluminum substructure from reaching temperatures above 177°C. Previous studies (Reference 1) have shown that multilayer insulations can achieve lower backface temperatures than fibrous silica (baseline) insulations of the same thickness. This fibrous silica (baseline) insulation, called Advanced Flexible Reusable Surface Insulation (AFRSI), has been described previously in detail (References 2,3) and is used extensively as a TPS on the Space Shuttle Orbiter. However, multilayer (MLI) insulations described previously (Reference 1) were not practical to use because of the heavy weight of the metal foils. The objective of this study was to determine the thermal efficiency of lighter composite insulations with a minimum or no weight penalty compared to fibrous silica (baseline) insulation.

In the present study, an aluminum foil 0.0025 cm thick was used in combination with a scrim cloth, which resulted in a 24% weight increase when using the composite insulation rather than the AFRSI. However, this weight penalty was eliminated entirely by the use of an aluminized polyimide film in the assembly.

A potential application for such multilayer insulations would be as a TPS system for the aerobraking of the Aeroassist Orbital Transfer Vehicle (AOTV). Depending on the exact location of the insulation, the insulation may experience a maximum heating rate of 0.5 W/cm^2 in the base region or 30 W/cm^2 in the forebody or stagnation region of the aerobrake. It should be noted, however, that the multilayer insulation would not be used in the area of highest heating rates. There, the maximum heating rate would be reached at approximately 100 sec into the heating pulse. The multilayer insulations exposed to lower heating rates would reach maximum backface temperature at approximately 400 sec, at which time the pressure would be essentially that of space. Multilayer insulations are intended for use in a space vacuum where gas conductivity between the foils is negligible and the overall effective thermal conductivity is very small. Because of this, appropriately designed multilayer insulations could operate efficiently within the heating and pressure environment of the AOTV and could provide a weight saving compared to other types of insulations.

2. DESIGN OF MULTILAYER INSULATIONS

The equation (Reference 4) that describes the heat transfer in multilayer insulations is as follows:

$$K_e = BK_sD_f^n + \frac{(r)^2G\,(T_F^2 + T_B^2)\,(T_F + T_B)t}{(a + 2s)\,(t/2) + (N - 1)\,[(2/E) - 1]} + \frac{(L)}{(L + I)}\,(K_g)$$

where

- a = absorption cross section,
- B = solid fraction in insulation,
- D_f = fiber diameter,
- E = emittance,
- G = Stefan-Boltzmann constant,
- K_e = effective thermal conductivity,
- K_s = thermal conductivity of solids,
- K_g = thermal conductivity of gas,
- L = cell length in insulation,
- I = mean free path of gas,
- N = number of metal foils,
- n = exponent,
- r = index of refraction,
- s = scattering cross section,
- T_F = temperature on front side,
- T_B = temperature on back side,
- t = thickness of insulation.

The above equation was used as a guide for the selection of materials and geometry of the composite insulations. It shows the importance of some of the properties of the components and geometry in the multilayer insulations. For example, to achieve a lower thermal conductivity in the entire system, a larger number of foils having a low emittance at elevated temperatures is preferred. The foils should be placed in the composite where T_F and T_B are relatively small. A small fiber diameter is preferable in the insulation and a low thermal conductivity in the components. For very low pressures, the mean free path of the gas is very large compared to the cell length, so the gas conduction term may be ignored. However, for moderate pressures this term can be significant. The multilayer insulation samples were fabricated on the basis of the above considerations and the previous results (Reference 1).

3. DESCRIPTION OF MATERIALS

A description of the different composite insulations is shown in Table 1. Configurations 1-4 had stainless steel foil as radiation shield material and configurations 5-8 had aluminum foil. The foil was separated by an aluminoborosilicate (ABS) scrim cloth in insulations 1-5, and 7, and by the insulation itself in 6 and 8. (The purpose of the scrim cloth was to eliminate heat shorts.) The two different configurations used are shown in Figures 1 and 2. The multilayer insulation (MLI) shown in Figure 1 uses metal foil separated by the scrim cloth, while in the variable multilayer insulation (VMLI) shown in Figure 2, the foils are separated by the insulation and no scrim cloth is used. Insulations 9 and 10 were the AFRSI. Insulation 11 contained 20 plies of aluminized polyimide (Kapton®) film as the radiation shield material. The film was composed of 700 Å of chemically vapor-deposited (CVD) aluminum on polyimide film 0.0012 cm thick. The use of this film eliminates the need for additional ceramic scrim material. In the composite insulations the metal foils act as the radiation shield in the multilayer assembly and must maintain their optical properties at high temperatures.

Infrared reflectance measurements were performed on the foils and the aluminized film over the wave region of 2.5 to 20.0 μm. The spectral reflectance of the foils and the aluminized film is shown in Figure 3. As it can be seen, the stainless steel before and after heating had a lower reflectance than the aluminum. There was only a small reduction in the reflectance of the aluminum foil after heating, and this reduction was fairly uniform throughout the wavelengths tested. The aluminized polyimide film, after heating at 500°C in air, had approximately the same reflectance as the nonheated aluminum foil.

The stainless steel foil in configurations 1-4 resulted in a 35-39% weight increase over the AFRSI of equivalent thickness, while the aluminum foil in configurations 5-8 resulted in a 24% weight increase over the AFRSI of equivalent thickness. When the scrim cloth was eliminated, as in configurations 6 and 8, there was no weight penalty.

The stainless steel foil or the 0.0025-cm-thick aluminum foil would not be suitable for flight because of the weight penalty. All of the above configurations contained nine layers of foil and nine layers of scrim cloth. Configuration 11 contained 20 layers of aluminized polyimide film, resulting in an overall density equal to the AFRSI insulation with no weight penalty.

The composite insulations were fabricated with a bottom and top ABS fabric. At higher heating rates, such as those to be encountered by the aero-assisted flight experiment (AFE), the top fabric would be replaced with silicon carbide fabric. In order to assess the effectiveness of different types of insulations, configurations 1-4 were fabricated with four different types of insulations. Composite insulation 1 contained a silica felt similar to the baseline insulation, with an average fiber diameter of 1.5 μm. The fibers were rather randomly oriented in the felt. Composite insulation 3 contained a silica mat with an average fiber diameter of 5 μm. The fibers were oriented in a configuration more planar than random. Insulation 2 contained an ABS (62% Al_2O_3, 24% SiO_2, 14% B_2O_3) mat with an average fiber diameter of 3.5 μm. Insulation 4 contained an alumina (95% Al_2O_3, 5% SiO_2) mat with an average fiber diameter of 3.5 μm. Composites 5-8 utilized either silica or ABS insulation, with the aluminum foil separated either by the scrim cloth or by the insulation itself. Composite 11 contained silica insulation. Composites 5 and 7 had the scrim cloth separating the foils, while variable multilayer insulations (VMLI) 6 and 8 had the foil separated by the insulation itself. All insulations were heat cleaned at 454°C in air for 2 hr to remove any sizing or organic coating from the fibers. Insulations 9 (1.0 cm thick) and 10 (2.4 cm thick) were both AFRSI.

4. TEST RESULTS

The thermal response, or backface temperature of the composite insulations was determined by using a procedure and apparatus described previously (Reference 5). The pressure used in the apparatus for testing configurations 1-10 was 20 mm Hg. The equipment was subsequently modified to test at a pressure of 1.5 mm Hg which simulates the vacuum environment of the AFE vehicle. Configuration 11 was tested at this lower pressure with the AFRSI 10. The heat pulse applied to the front surface is shown in Figure 4. The backface temperature was measured for 20 min.

The test results were the average of eight test runs from each configuration. Two thermocouples were used to determine the top temperatures: one embedded in a reaction cured glass (RCG) coating on the top of the sample holder shown in Figure 5; and the second uncoated thermocouple located below the top fabric of the insulation. The thermocouple below the fabric averaged 13°C below the RCG thermocouple at the maximum temperature.

Figures 6 and 7 show the thermal responses of 1.0-cm-thick composite insulations 1-4 (with stainless steel foil) compared to the AFRSI 9 of equivalent thickness. Figure 6 shows that composite 1 (containing the silica felt with the 1.5 μm fiber) had the lowest backface temperature. It was followed by composite 2 (containing the ABS mat) and the AFRSI 9. It should be noted that the ABS mat had only a slightly higher backface temperature than the silica insulation, which could be attributed to its larger

fiber diameter. Figure 7 shows that composite insulation 4 (containing the alumina insulation) had a backface temperature similar to the AFRSI 9. This insulation had the highest backface temperature of all the MLI insulations tested, and this could be attributed to its higher thermal conductivity. Composite insulation 3 contained the silica mat with the 5 μm diameters fibers. This insulation reached a maximum backface temperature of 315°C compared to 300°C for the silica insulation shown in Figure 6. This is attributed to the higher diameter of the fiber.

Figures 8, 9, and 10 are comparisons of the 2.4-cm-thick aluminum foil composite insulation with the AFRSI of equivalent thickness. Figure 8 shows a comparison of the AFRSI 10 and the MLI and VMLI geometries with the same silica felt. There is no significant difference in the thermal performance of the two geometries. However, in the VMLI configuration, the top aluminum foil melted because of its proximity to the top surface and heat source. Therefore, this type of configuration is impractical to use. Figure 9 is a comparison of the AFRSI 10 with the silica and ABS insulations in the MLI geometry. Both of the MLI configurations had lower backface temperatures than the monolithic AFRSI. Figure 10 compares the same two types of insulation in the VMLI geometry. There was no significant difference between the two types of insulations. This could be attributed to the higher efficiency of the aluminum foils as a reflective shield which diminished any small differences in the thermal efficiency of the insulations.

Figure 11 is a comparison of the AFRSI 10 and MLI 11 containing the aluminized polyimide film. Both insulations were 2.4 cm thick. Twenty layers of the film were placed on the bottom of the insulation in this configuration. The 0.0012-cm-thick polyimide film has a relatively high transparency in the far infrared and near infrared region (Reference 7) so it was necessary to have an aluminum coating of sufficient thickness to have relatively low emittance in order to provide efficient radiation shielding. The aluminum coating was chemically vapor-deposited (CVD) and was approximately 700 Å thick. No damage to the film was observed after repeated test runs. When the film was subjected to the heat cleaning cycles of the insulation at 454°C, no degradation was observed. However the film was slightly curled because of the difference in the thermal expansion coefficients of the aluminum and the polyimide film. This should not impose a severe problem in the insulation blankets since they are sewn in a quilted configuration.

The thermogravimetric analysis of the aluminized film is shown in Figure 12. The oxidative degradation of the film was initiated at approximately 500°C. The advantage of the use of this film was the weight reduction. The film weighs approximately 18 g/m^2. The thinnest aluminum foil commercially available is 0.00076 cm thick and weighs 20 g/m^2. When combined with a thin ceramic scrim cloth, the total weight is 46 g/m^2. A comparison study of thermal performance versus weight is required in order to determine the optimum configuration.

5. DATA ANALYSIS

The data shown in Figures 8 and 9 were analyzed by using a specially developed, one-dimensional heat transfer model similar to the one described in Reference 1. The numerical model simulated the composite insulation test sample shown in Figure 1 when mounted in its test fixture. This fixture and the test environment were also described in Reference 1. For the test, the top surface of the sample was maintained at a temperature of about 1070°C for 2 min and then allowed to cool as shown by the measured temperature profile in Figure 4. The transient, backface temperature of this sample was measured. These backface temperatures were used in the correlation procedure shown in Figure 13. First, an iteration procedure was used to determine the thermal conductivity of the baseline insulation material, which was the same as that used in the composite insulation samples that were analyzed. Then this conductivity was used in a second iteration procedure to determine the effective thermal conductivity of the multilayer insulation component. These thermal conductivity variations were made by applying factors to the temperature-dependent thermal conductivity of AFRSI (References 2,3). This assumes a shape for the temperature dependency curve, but most ceramic insulations of the current class exhibit similar variations with temperature. To allow an arbitrary shape to these curves would be prohibitively time consuming.

The numerical model consists of 30 nodes representing the insulation, 1 node for each multilayer insulation layer, 1 node each for the top and bottom cloth surfaces, 4 nodes for the aluminum disk thermocouple mount, and 10 nodes representing the insulation between the sample and the water-cooled base of the test facility.

The results of the analysis of the data presented in Figures 6 and 9 are summarized in Figures 14 and 15, respectively. The three circles in each of these figures are backface temperatures for the baseline model calculated by using the correlating thermal conductivities obtained from the first iteration procedure in Figure 13. For Figure 14 the correlating insulation conductivity differs from that of AFRSI by a factor of 0.96, and for Figure 15 the factor is 1.05. For graphical purposes, only these numbers have been rounded to 1.0 in Figure 14. This is reassuring because the insulation used in these silica samples is essentially the same as AFRSI. The dashed curves in these figures represent the calculated effect of adding the multilayer insulation component while maintaining the overall sample thickness. For the factor = 1 curve, the effective conductivity of the multilayer insulation component is the same as that of the insulation. The difference in temperature from the baseline is then the result of the higher thermal mass of the multilayer insulation. The differences between these curves and the other dashed curves show the effect of reducing the multilayer insulation conductivity from that of AFRSI in the calculations. For the stainless steel composite insulation sample in Figure 14, the data are best correlated by an effective multilayer insulation conductivity that is about 0.7 times that of AFRSI. For the aluminum composite insulation sample, shown in Figure 15, this factor is about 0.6. This difference is within the reliability of the analysis. The thermal conductivity of air is approximately 60% that of AFRSI. Because of this lower thermal conductivity, the composite insulation containing aluminum will be utilized as an experimental TPS on the aerobrake of the AOTV.

6. CONCLUSIONS

Multilayer insulations consisting of alternating metal foils and scrim cloth or aluminized polyimide film were evaluated for thermal performance. These composite flexible insulations were compared to the Advanced Flexible Reusable Surface Insulation (AFRSI). The principal results obtained were as follows:

1. The 2.4-cm-thick AFRSI reaches a backface temperature of approximately 160-170°C at 15 min, when tested at 20 mm Hg pressure and in accordance with the procedures described. The composite insulation, with the ABS-Al layers alternating with either silica or ABS insulation, reaches 110-130°C backface temperature at equivalent time. The weight penalty for these composite insulations is approximately 24%.
2. The composite insulation, consisting of aluminized polyimide film with silica insulation, reaches a backface temperature of 110°C at 15 min when tested at 1.5 mm Hg pressure. The AFRSI at equivalent thickness and density reaches a backface temperature of 145°C at 15 min.
3. The spectral reflectance of the aluminum as a foil, or chemically vapor-deposited on polyimide film, does not degrade

significantly as a function of temperature. The high reflectance of these films makes them attractive as radiation shields.

4. Comparative results were obtained between the one-dimensional numerical heat transfer model and some of the experimental data. The model can be used to predict the heat transfer properties of the composite insulations and to estimate their thermal conductivity properties.

5. The effectiveness of the multilayer component increases as a function of overall thickness of the insulation. The multilayer insulations were most effective in the 2.4-cm-thick configuration.

6. The numerical mode indicates that lower thermal conductivity can be attained in the aluminum composite flexible insulation than in the AFRSI. In addition, the composite insulation containing the aluminized film could provide weight reduction as a TPS for aerospace vehicles such as the AOTV.

Acknowledgment: One of the authors (W. C. P.) was supported by a grant from NASA to Eloret Institute (NCC2-434).

References

1. Kourtides, D. A.; Pitts, W. C.; Araujo, M.; and Zimmerman, R. S.: "High Temperature Properties of Ceramic Fibers and Insulations for Thermal Protection of Atmospheric Entry and Hypersonic Cruise Vehicle," SAMPE Quarterly, Vol. 19, No. 3, Apr. 1988.
2. Goldstein, H.; Leiser, D.; Larson, H.; and Sawko, P. M.: "Improved Thermal Protection System for the Space Shuttle Orbiter," AIAA Paper 82-0630, May 1982.
3. Sawko, P. M.: "Effect of Processing Treatments on Strengths of Silica Thread for Quilted Ceramic Insulation on Space Shuttle," SAMPE Quarterly, Vol. 16, No. 4, July 1985, pp. 17-21.
4. Viskantan, R.: "Heat Transfer by Conduction and Radiation in Absorbing and Scattering Materials," G. Heat Transfer (ASME), 1965.
5. ASTMC-177-85: "Steady State Heat Flux Measurements and Thermal Transmission Properties by Means of the Guarded Hot Plate Apparatus."
6. Smith, M.: "Thermal Diffusivity Apparatus," NASA Tech Brief 10642, Ames Research Center, Jan. 1979.
7. Cunnington, G. R.; Zierman, C. A.; and Funai, A. I.: "Performance of Multilayer Insulation Systems for Temperatures to 700°C," NASA CR-907, Oct. 1967.

Table 1. Description of insulations.

CONFIGURATION TYPE AND NUMBER	TOP/BOTTOM FABRIC	INSULATION TYPE	SPACER	REFLECTIVE SHIELD FOIL	THICKNESS, cm	DENSITY, g/cm^3
MLI 1	ALUMINOBORO-SILICATE (ABS)	SILICA FELT	ABS SCRIM	STAINLESS STEEL(S.S.)	1.0	0.28
MLI 2	ABS	ABS MAT	ABS SCRIM	S.S.	1.0	0.28
MLI 3	ABS	SILICA MAT	ABS SCRIM	S.S.	1.0	0.28
MLI 4	ABS	ALUMINA MAT	ABS SCRIM	S.S.	1.0	0.28
MLI 5	ABS	SILICA FELT	ABS SCRIM	ALUMINUM	2.4	0.17
VMLI 6	ABS	SILICA FELT	SILICA FELT	ALUMINUM	2.5	0.14
MLI 7	ABS	ABS FELT	ABS SCRIM	ALUMINUM	2.4	0.16
VMLI 8	ABS	ABS FELT	ABS FELT	ALUMINUM	2.5	0.14
AFRSI 9	SILICA	SILICA FELT	NONE	NONE	1.0	0.21
AFRSI 10	SILICA	SILICA FELT	NONE	NONE	2.4	0.13
MLI 11	ABS	SILICA FELT	POLYIMIDE FILM	ALUMINUM (CVD)	2.4	0.13

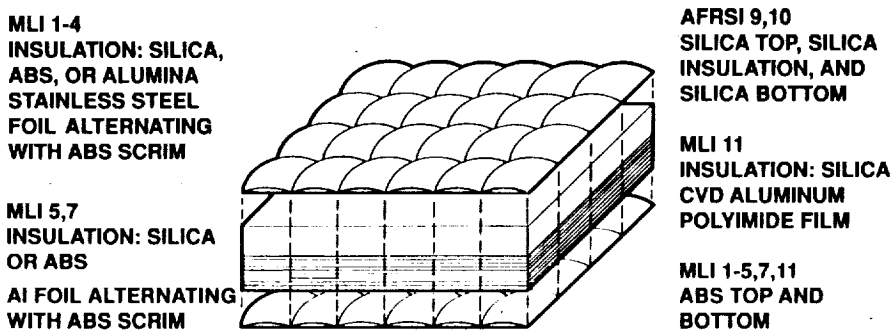

Figure 1. Configuration of multilayer composite insulation.

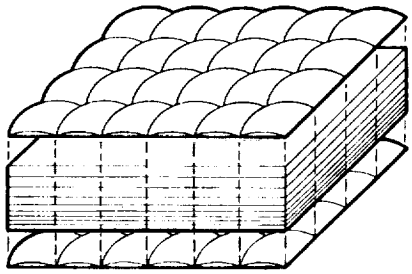

Figure 2. Configuration of variable multilayer composite insulation.

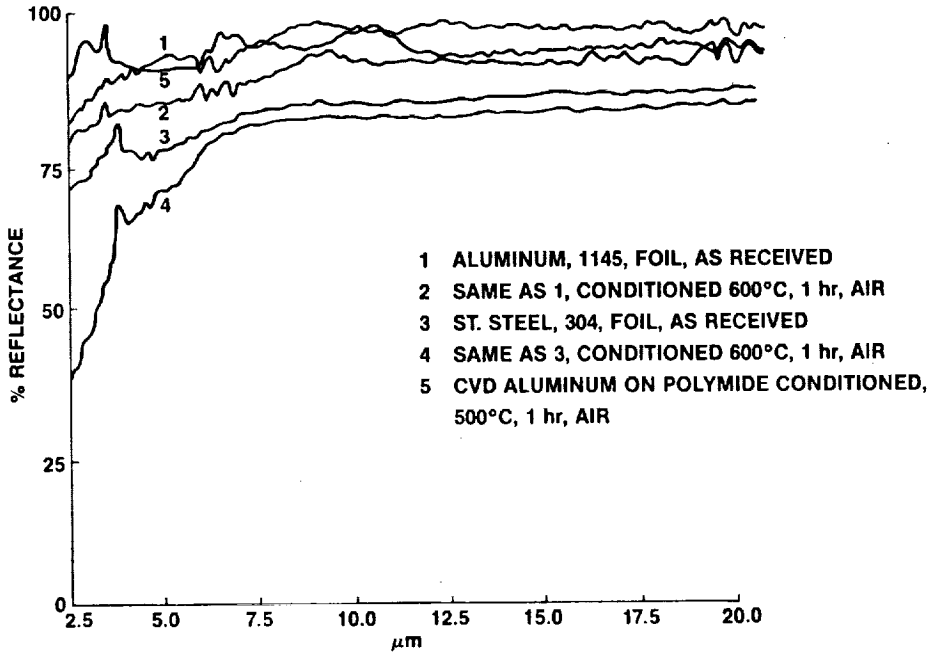

Figure 3. Reflectance of stainless steel foil, aluminum foil, CVD aluminum on polyimide film before and after heating in air.

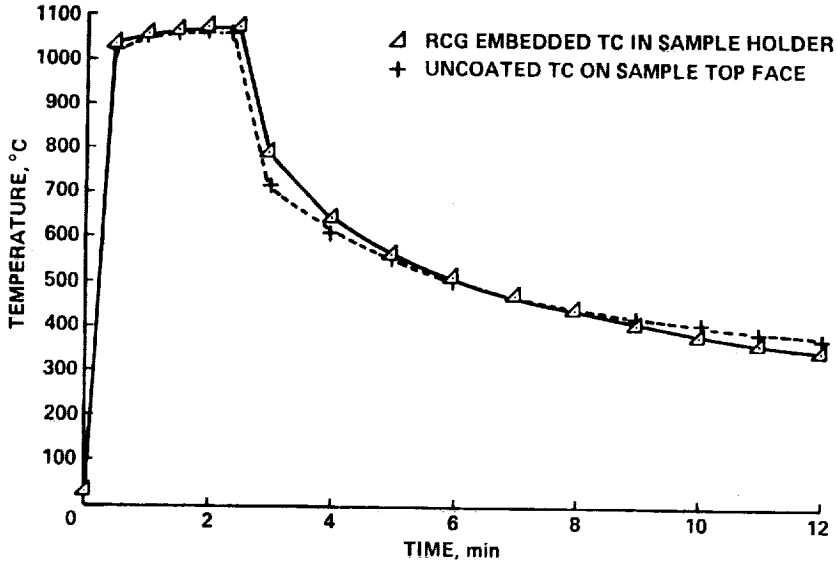

Figure 4. Temperature comparison of surface thermocouples (TC) embedded in RCG and in insulation fabric.

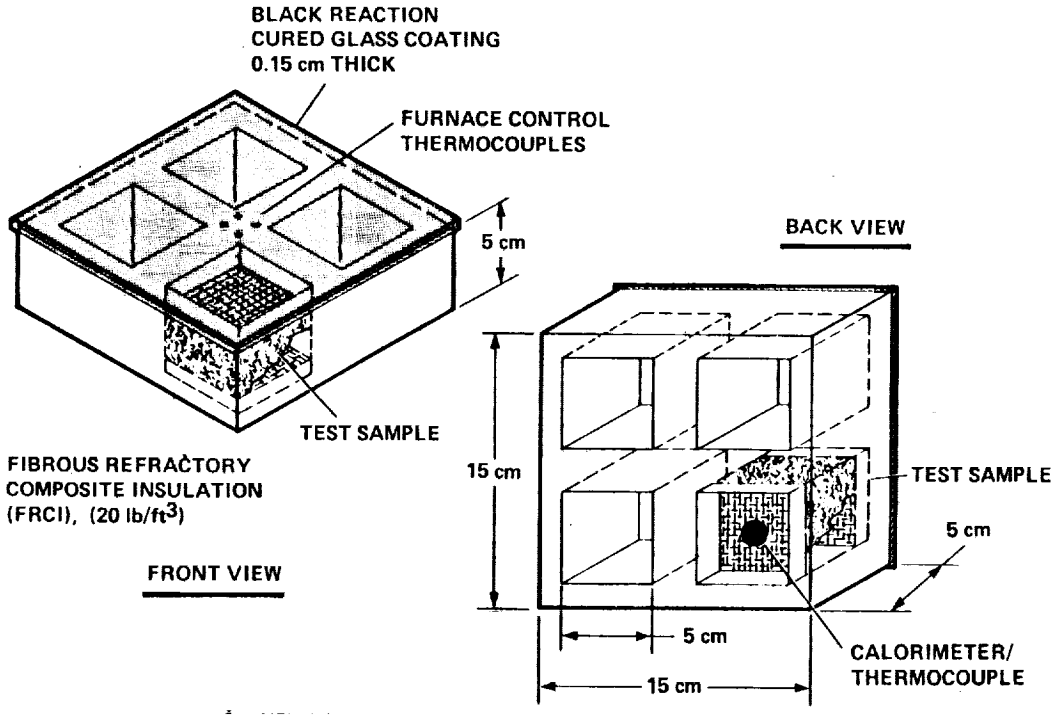

Figure 5. Thermal diffusivity sample holder with test sample in position.

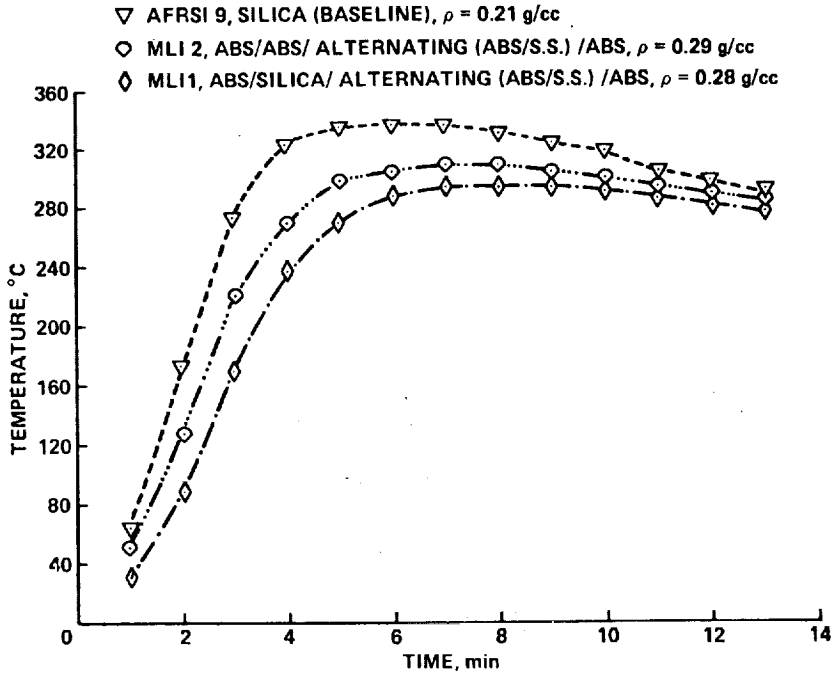

Figure 6. Comparison of thermal response of stainless steel-silica felt or aluminoborosilicate multilayer insulations with silica insulation.

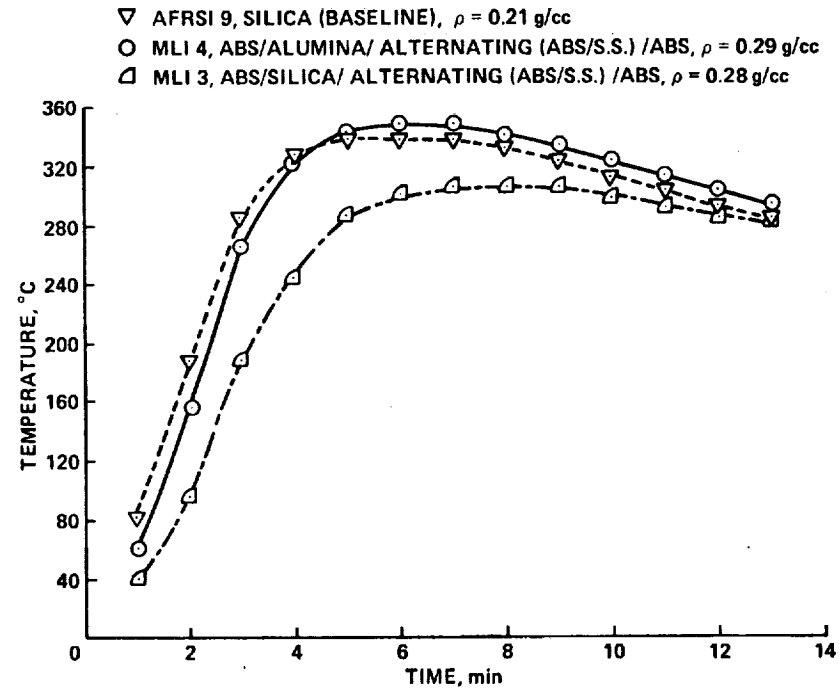

Figure 7. Comparison of thermal response of stainless steel-silica mat or alumina multilayer insulations with silica insulation.

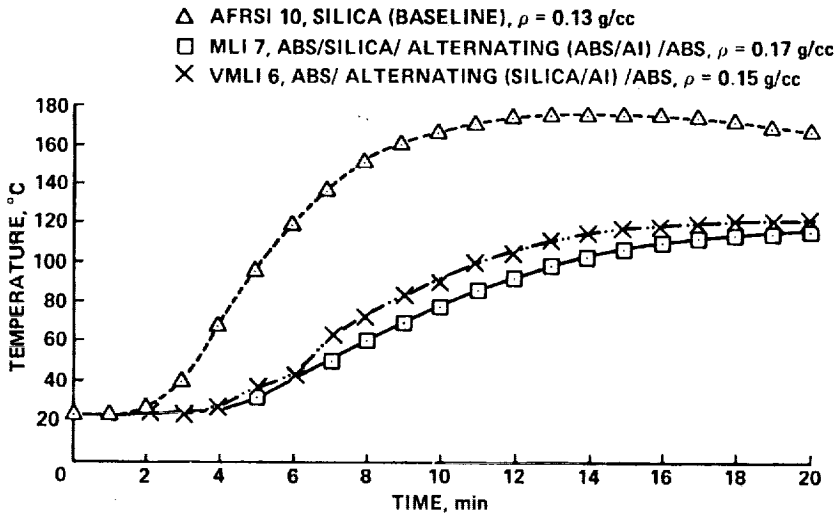

Figure 8. Comparison of thermal response of aluminum-silica felt multilayer or variable MLI insulations with silica insulation.

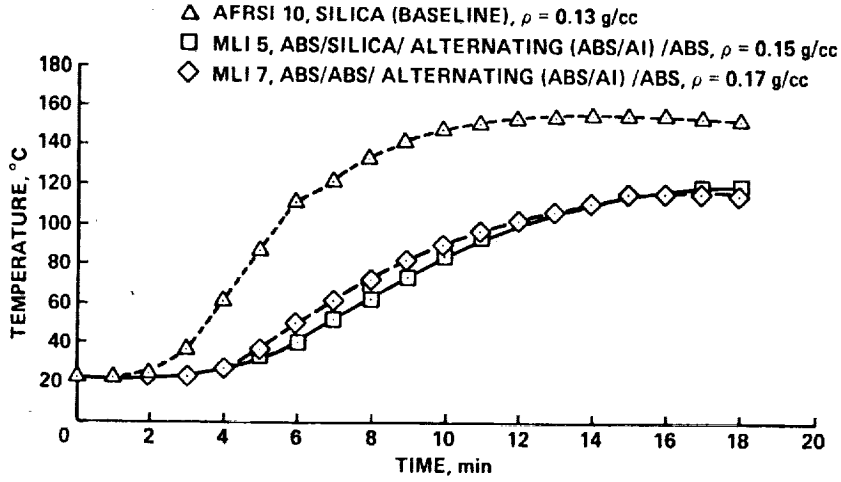

Figure 9. Comparison of thermal response of aluminum-silica felt or aluminoborosilicate multilayer insulations with silica insulation.

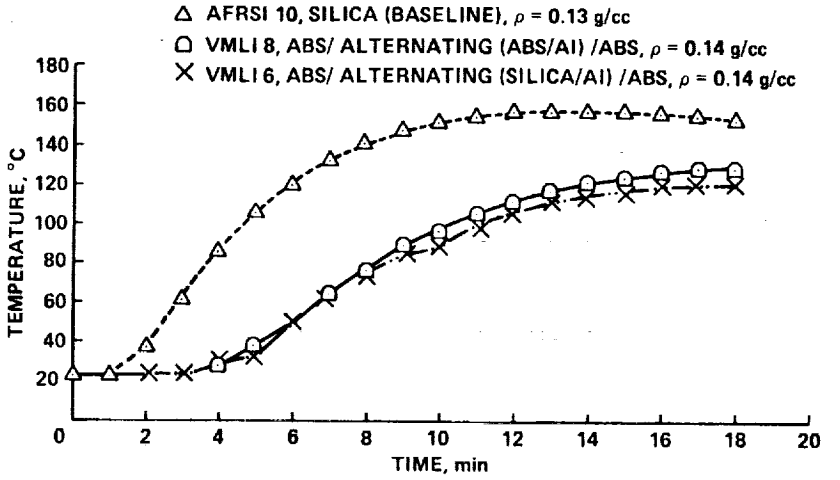

Figure 10. Comparison of thermal response of aluminum-silica felt or aluminoborosilicate variable multilayer insulations with silica insulation.

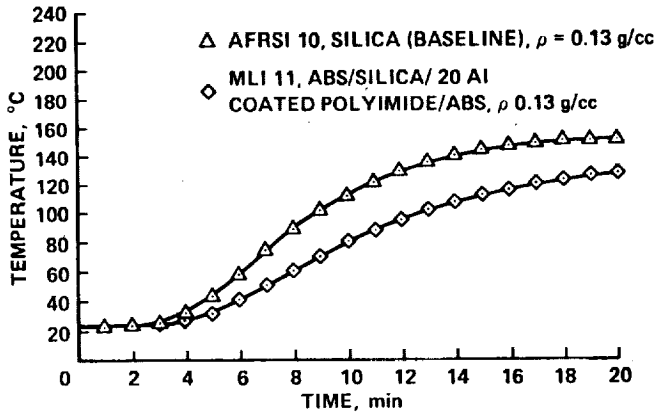

Figure 11. Comparison of thermal response of aluminized polyimide-silica felt multilayer insulation with silica insulation.

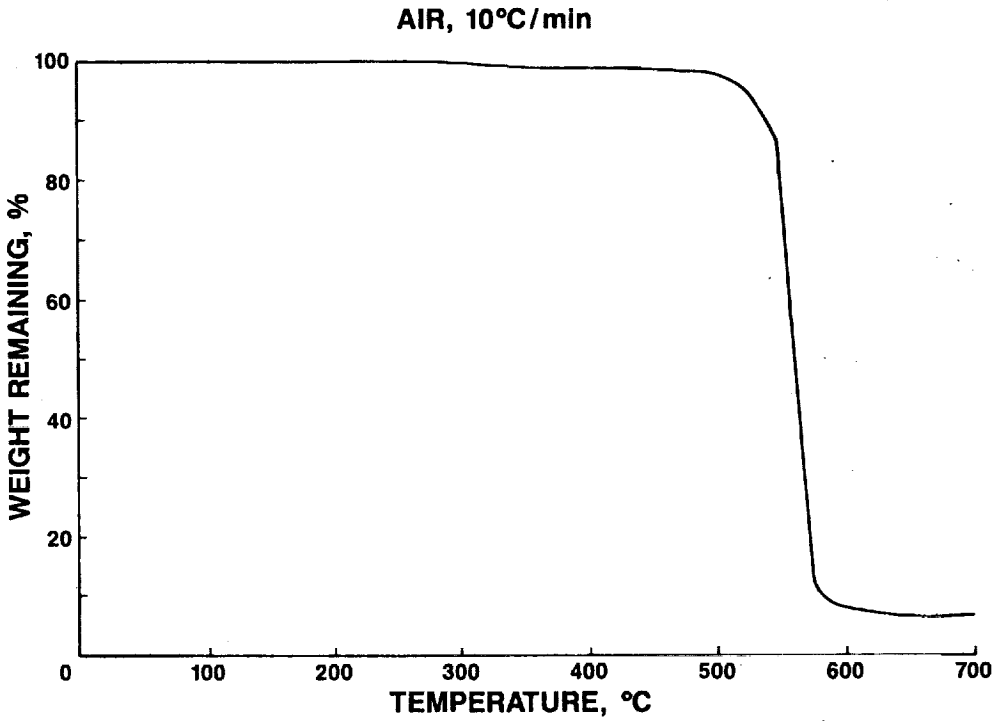

Figure 12. Thermogravimetric analysis of aluminized polyimide film.

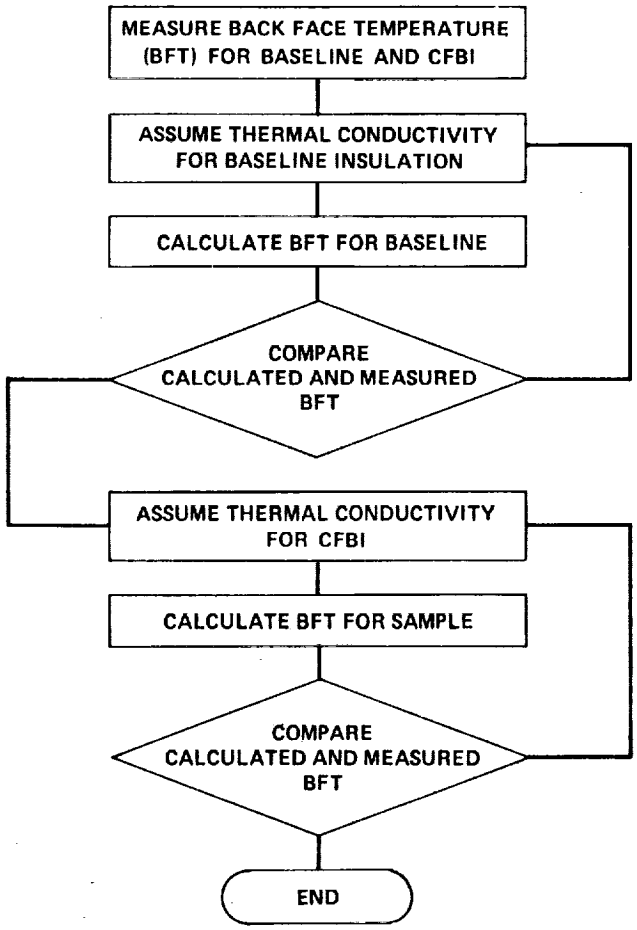

Figure 13. Data analysis procedure used for calculations shown in Figures 14 and 15.

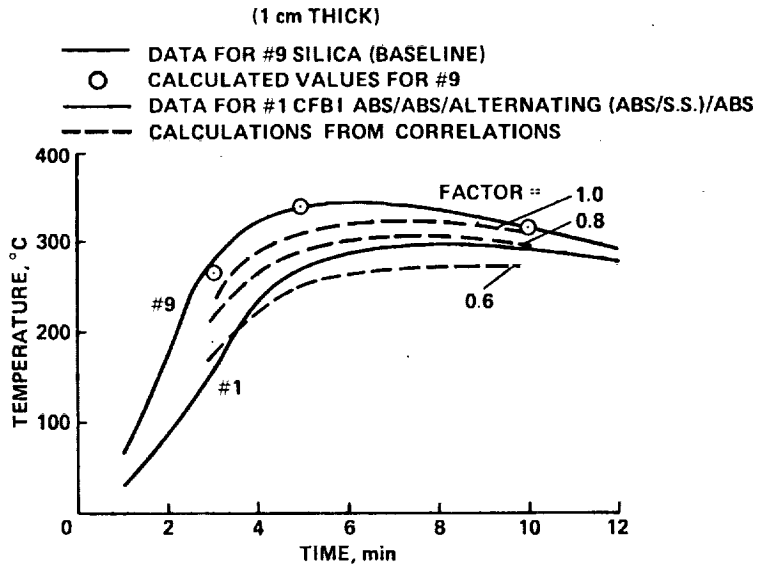

Figure 14. Comparison of experimental data with calculated values for Configurations Nos. 1 and 9.

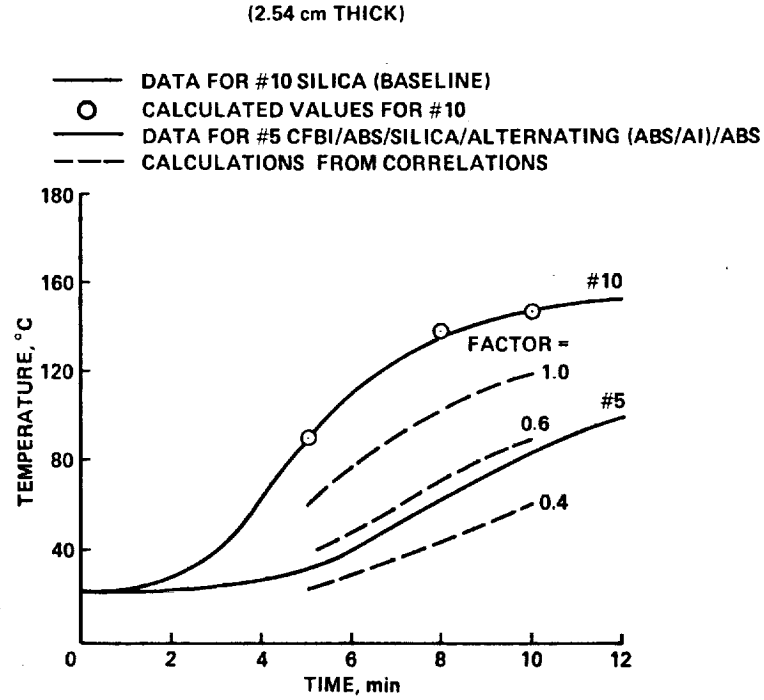

Figure 15. Comparison of experimental data with calculated values for Configurations Nos. 5 and 10.

NASA
National Aeronautics and Space Administration

Report Documentation Page

1. Report No.	2. Government Accession No.	3. Recipient's Catalog No.
NASA TM-101071		

4. Title and Subtitle

Composite Multilayer Insulations for Thermal Protection of Aerospace Vehicles

5. Report Date

February 1989

6. Performing Organization Code

7. Author(s)

D. A. Kourtides and W. C. Pitts (Eloret Institute, Sunnyvale, CA)

8. Performing Organization Report No.

A-89035

10. Work Unit No.

506-43-31

9. Performing Organization Name and Address

Ames Research Center
Moffett Field, CA 94035

11. Contract or Grant No.

13. Type of Report and Period Covered

Technical Memorandum

12. Sponsoring Agency Name and Address

National Aeronautics and Space Administration
Washington, DC 20546-0001

14. Sponsoring Agency Code

15. Supplementary Notes

Point of Contact: D. A. Kourtides, Ames Research Center, MS 234-1, Moffett Field, CA 94035
(415) 694-4784 or FTS 464-4784

Presented at the "Composites in Manufacturing 8" Exposition and Conference, Society of Manufacturing Engineers, Anaheim, CA, January 9-12, 1989

16. Abstract

Composite flexible multilayer insulation systems (MLI), consisting of alternating layers of metal foil and scrim cloth or insulation quilted together using ceramic thread, were evaluated for thermal performance and compared with a silica fibrous (baseline) insulation system. The systems studied included (1) alternating layers of aluminoborosilicate (ABS) scrim cloth and stainless steel foil, with silica, ABS, or alumina insulation; (2) alternating layers of scrim cloth and aluminum foil, with silica or ABS insulation; (3) alternating layers of aluminum foil and silica or ABS insulation; and (4) alternating layers of aluminum-coated polyimide placed on the bottom of the silica insulation. The MLIs containing aluminum were the most efficient, measuring as little as half the backface temperature increase of the baseline system.

17. Key Words (Suggested by Author(s))	18. Distribution Statement
Composites Insulation Thermal protection	Unclassified – Unlimited Subject category – 24

19. Security Classif. (of this report)	20. Security Classif. (of this page)	21. No. of pages	22. Price
Unclassified	Unclassified	14	A02

For sale by the National Technical Information Service, Springfield, Virginia 22161